ISSN 0101 3084

CNEN/SP

ipen Instituto de Pesquisas Energéticas e Nucleares

GOVERNO DO BRASIL

DESCRIPTION OF THE MONTE CARLO CODE FOR THE RESPONSE CALCULATION OF THE DUAL THIN SCINTILLATOR (DTS) NEUTRON DETECTOR

Mauro da Silva DIAS

IPEN Pub 397

OUTUBRO/1993

SÃO PAULO

IPEN Pub 397 OUTUBRO/1993

DESCRIPTION OF THE MONTE CARLO CODE FOR THE RESPONSE CALCULATION OF THE DUAL THIN SCINTILLATOR (DTS) NEUTRON DETECTOR

Mauro da Silva DIAS

SERVIÇO DE PROTEÇÃO RADIOLÓGICA

CNEN/SP
INSTITUTO DE PESQUISAS ENERGÉTICAS E NUCLEARES
SÃO PAULO BRASIL

Série PUBLICAÇÃO IPEN

INIS Categories and Descriptors

E41 00
F50 00

MONTE CARLO METHOD
SCINTILLATION COUNTERS
NEUTRON DETECTORS
RESPONSE FUNCTIONS
PERFORMANCE

IPEN Doc-4867
Aprovado para publicação em 10/05/93
Nota: A redação, ortografia, conceitos e revisão final são de responsabilidade do(s) autor(es)

DESCRIPTION OF THE MONTE CARLO CODE FOR THE RESPONSE CALCULATION OF THE DUAL THIN SCINTILLATOR (DTS) NEUTRON DETECTOR

Mauro da Silva DIAS
COMISSÃO NACIONAL DE ENERGIA NUCLEAR - SP
INSTITUTO DE PESQUISAS ENERGÉTICAS E NUCLEARES
CAIXA POSTAL 11049, PINHEIROS
05422-970 - SÃO PAULO - BRASIL

ABSTRACT

A detailed description and performance of the Monte Carlo code called CARLO DTS, developed for the efficiency and proton recoil spectra calculation of the Dual Thin Scintillator (DTS) neutron detector is given The code CARLO DTS covers the neutron energy range between 1 and 20 MeV The cross sections and angular distributions were taken from the ENDF/B-V data file for the nuclear reactions involved H(n,n)H, C(n,n)C and inelastic scattering, (n,α), (n,n')3α reactions on carbon-12 Updated values from the ENDF/B-VI are considered for the H(n,n)H reaction cross section The theoretical calculations are compared to experimental results at two neutron energies, namely: 2 446 and 14 04 MeV, obtained by means of the Time Correlated Associated Particle Technique

DESCRIÇÃO DO CÓDIGO DE MONTE CARLO PARA O CÁLCULO DA RESPOSTA DO DETECTOR DE NÊUTRONS CINTILADOR FINO DUAL (DTS)

Mauro da Silva DIAS
COMISSÃO NACIONAL DE ENERGIA NUCLEAR - SP
INSTITUTO DE PESQUISAS ENERGÉTICAS E NUCLEARES
CAIXA POSTAL 11049, PINHEIROS
05422-970 - SÃO PAULO - BRASIL

RESUMO

Este trabalho apresenta uma descrição detalhada e o desempenho de um código de Monte Carlo denominado CARLO DTS, desenvolvido para o cálculo da eficiência e espectro de altura-de-pulso do detector de nêutrons: Cintilador Fino Dual (DTS) O código CARLO DTS cobre o intervalo de energia de nêutrons entre 1 e 20 MeV As secções de choque e distribuições angulares foram extraídas dos arquivos ENDF/B-V para as reações envolvidas: H(n,n)H, C(n,n)C, espalhamento inelástico e reações(n,α), (n,n')3α e C(n,n')3α no carbono-12 Valores atualizados do arquivo ENDF/B-VI foram considerados para a reação H(n,n)H Os cálculos teóricos foram comparados aos resultados experimentais em duas energias de nêutron, a saber: 2,446 e 14,04 MeV, obtidos por meio do método da Partícula Associada Correlacionada no Tempo

1 INTRODUCTION

The Monte Carlo code CARLO DTS, developed for the efficiency and proton recoil spectra calculation of the DUAL THIN SCINTILLATOR (DTS) neutron detector is described. Complete details about the DTS characteristics and performance are given in refs [2,3,4]

A schematic diagram of the detector is shown in Fig 1 It consists of two cylindrical pieces of NE-110 plastic scintillator 0 254 cm thick, 4 70 and 4 90 cm in diameter, respectively Each scintillator was coupled to a pair of RCA 8850 phototubes in head-on geometry Perspex light guides are used, with the same thickness as the scintillators As a result, most of the light that reaches the photocathode is by total internal reflection Each scintillator was wrapped in a 6 6 μm thick aluminum foil, except at the interface between the two scintillators, where a 0 66 μm thick aluminum foil was used The phototubes and scintillators were held together inside of a box which has a 54 μm thick aluminum window on each side, in order to make the system light tight

The code CARLO DTS covers the neutron energy range between 1 and 20 MeV The use of the detector described above between 15 and 20 MeV can be accomplished by changing the thickness of the second scintillator to about 0 40 cm

The development of the code CARLO DTS, suitable for the DUAL THIN SCINTILLATOR (DTS) neutron detector, started with the code CARLO BLACK [15] developed to be used for the BLACK NEUTRON DETECTOR efficiency and proton recoil spectra determination, at the Argonne National Laboratory This code has been taken as a basis because it was being used routinely at the National Institute of Standards and Technology (NIST) at the time the DTS detector was developed and because it has several routines which are similar to those developed for the DTS neutron detector

As described in ref [15], the principle of the

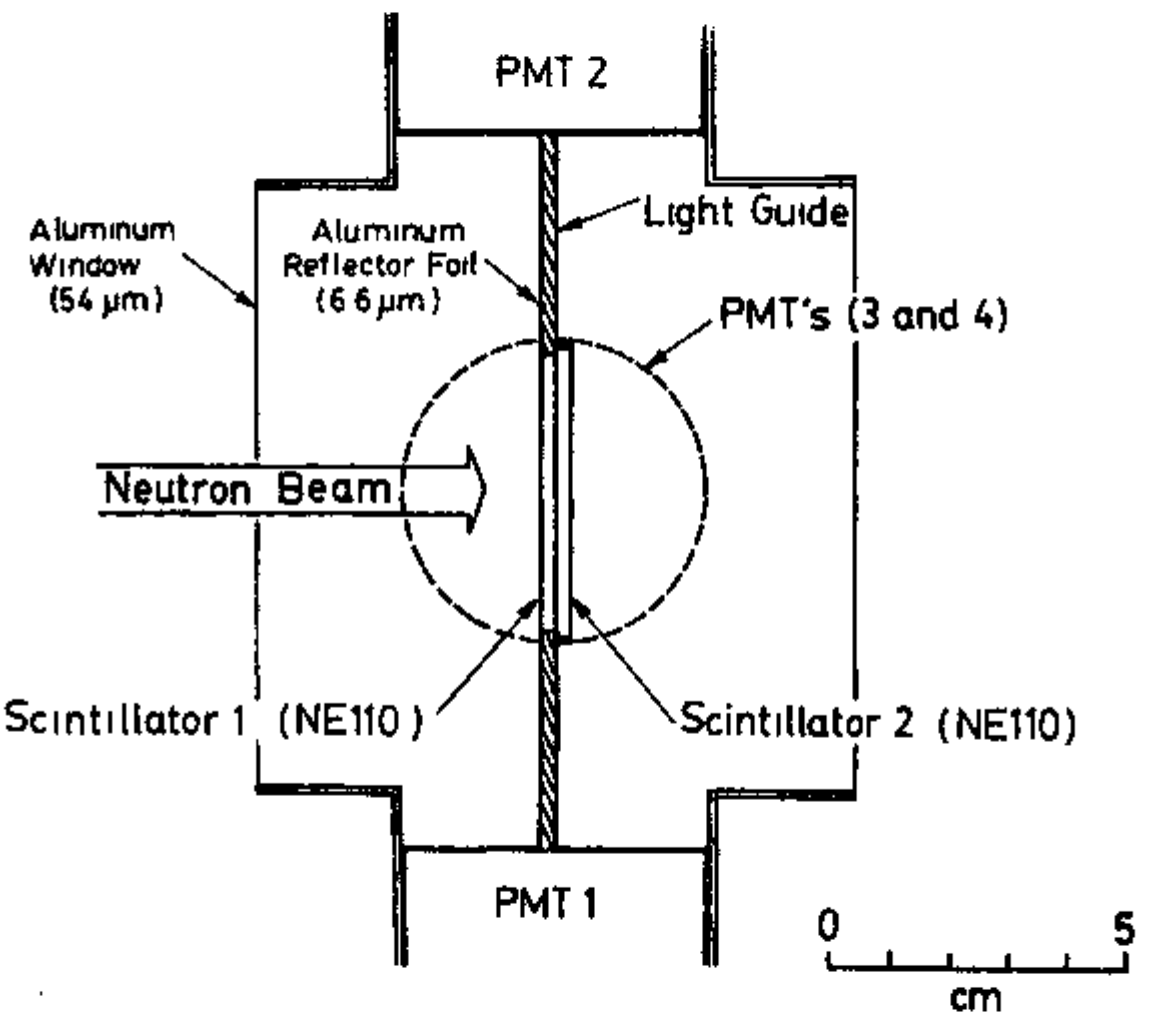

FIGURE 1 - Geometry of the Dual Thin Scintillator neutron detector

operation of the BLACK NEUTRON DETECTOR is very different as compared to the DTS neutron detector. For this reason, although the original program structure has been mantained, a great deal of modifications had to be introduced in order to update the code and fit it to the DTS detector characteristics.

The block diagram of the CARLO DTS code is shown in fig 2 The most relevant details on this code are described in the following sections Some aspects which were kept the same as the original code are omitted and can be seen in ref [15]

2 GENERAL FEATURES OF THE CODE CARLO DTS

The code CARLO DTS consists of a main program and fifteen subroutines Twelve of these subroutines have been modified with respect to the original ones and two of them, namely CHANX and LEADR, were eliminated since they refer to aspects of the BLACK NEUTRON DETECTOR geometry which are nonexistent in the DTS detector

The detector parameters and the coordinate system orientation are shown in figure 3 The detector is considered as a cylinder of height H_T and radius R, filled with scintillator containing hydrogen and carbon of concentrations N_H and N_C, respectively The neutron beam, with a radius R_B, is assumed to be homogeneous and normally incident to the detector frontface Nonhomogeneity or other incidence angles may be introduced by changing subroutine SOURCE according to the case of interest

The cylindrical regions where the scintillators 1 and 2 are located are called ZONES 1 and 2, respectively ZONE 3 is located outside the scintillators The contribution of the perspex light guide in the detector response is not considered It has been estimated to be negligible for neutron beam diameters much smaller than the detector diameter [3] Easy modifications can be introduced

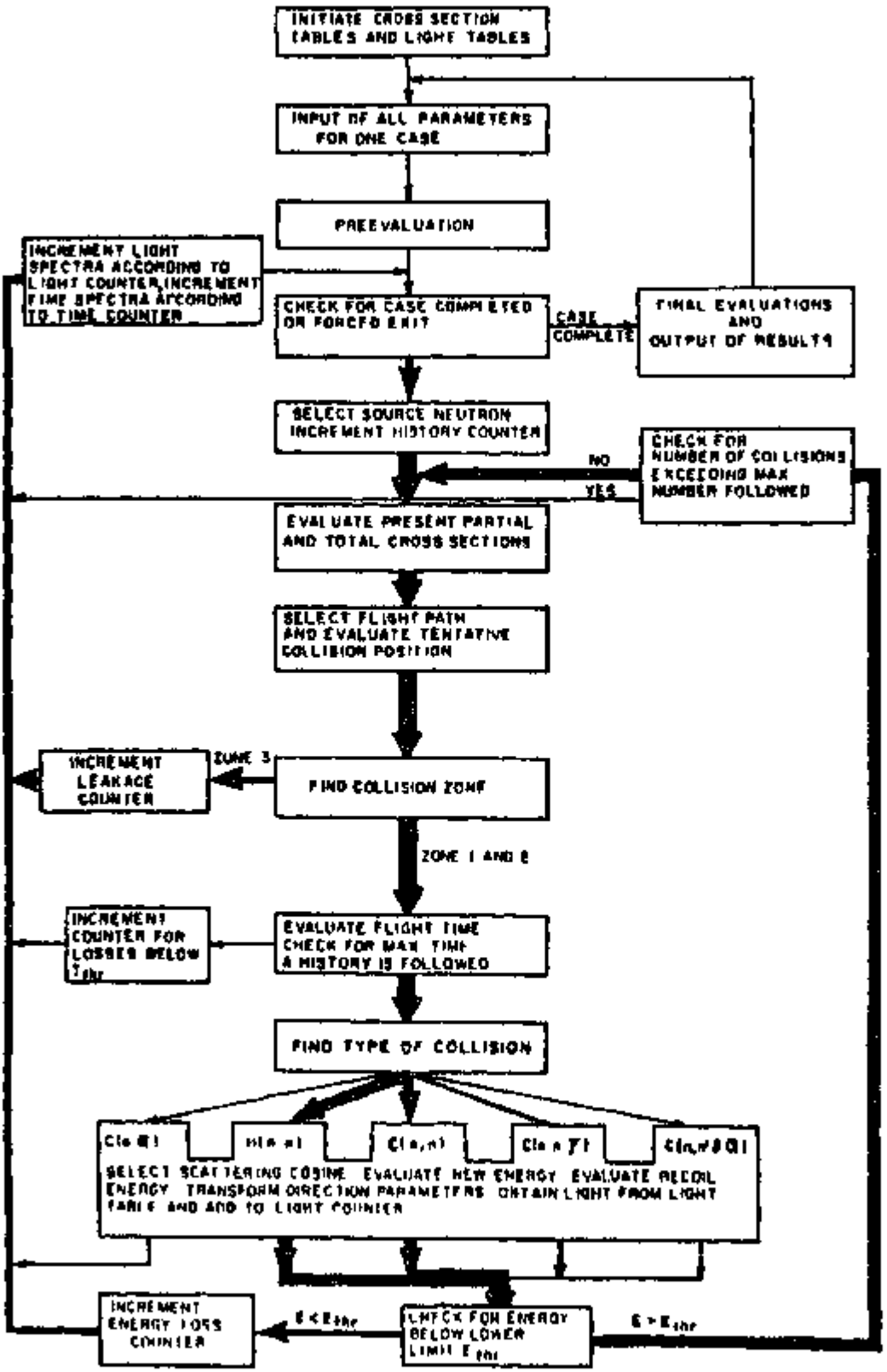

FIGURE 2 - Block Diagram of the code CARLO DTS

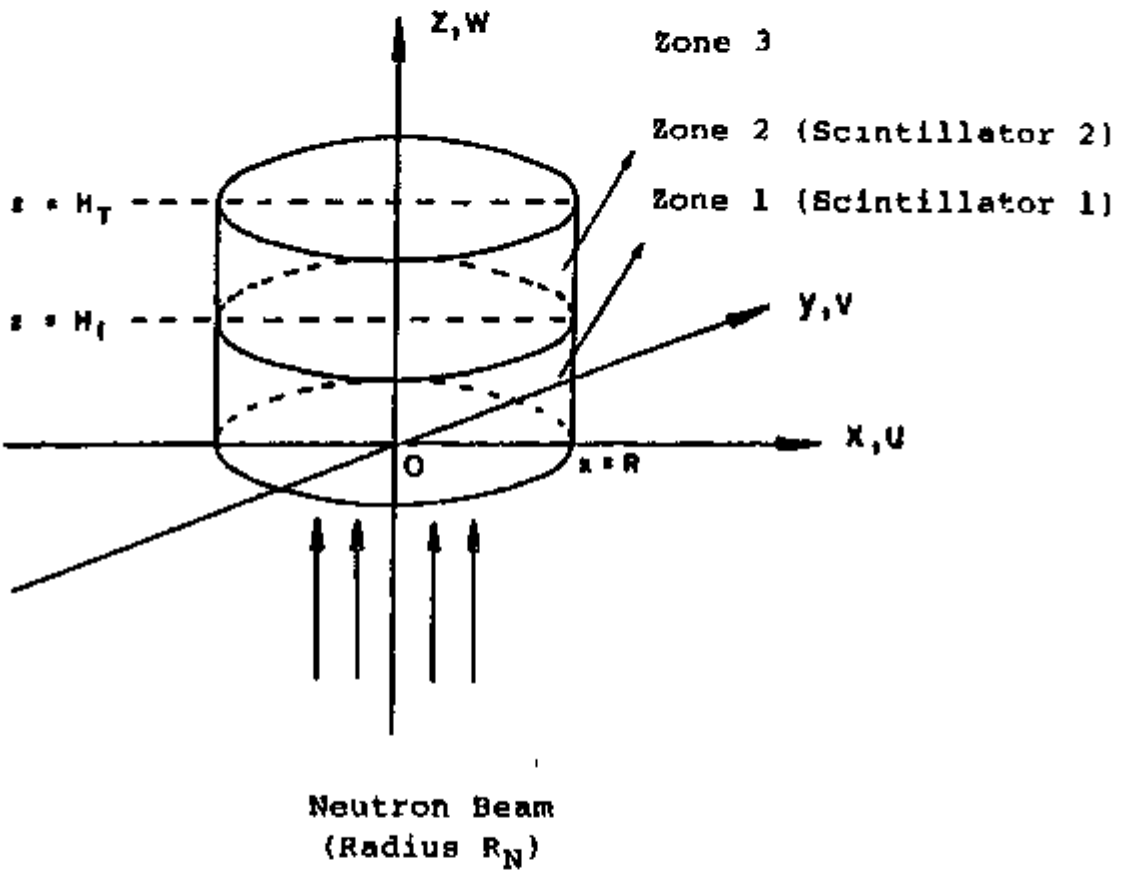

FIGURE 3 - Coordinate system ZONE 3 is the region outside the scintillators

in the code to calculate the response for neutron beams comparable or larger than the scintillators The neutron "history" is followed until it escapes from the system, falls below a specified threshold energy E_{thr}, or remains in the system more than an specified threshold time T_{thr} The light yields produced by the recoil particles or reaction products are added during the neutron trajectory and registered at the end of its "history".

The frequency in the path travelled by the neutron is indicated in figure 2 by the arrow thickness In more frequent paths fast calculation techniques or forced neutron collision were used in order to reduce the processing time Because the scintillators are thin, a neutron with energy in the range of 1 to 15 MeV will have, on the average, only one collision inside the detector The maximum number of collisions is below nine and the majority of neutrons escape the detector before being absorbed

To achieve a statistical uncertainty around 0 4 % about 10^6 histories are necessary, applying the forced collision technique Good pulse height distributions are obtained with about 4×10^5 histories

3 DESCRIPTION OF THE CODE CARLO DTS CALCULATIONS

This section describes the main features of the calculation performed by the code CARLO DTS The aspects which differentiate the code CARLO DTS as compared to the original code CARLO BLACK are emphasized Some usual aspects of the technique like coordinate transformation are omitted and can be seen in reference [15]

First, the parametrization of the nuclear reaction cross sections and kinematics are introduced Then, the forced collision technique is described and considerations are made on the light response tables for the recoil charged particles Finally, the corrections for lost coincidences and geometrical variation in the light collection are

presented

3 1 REACTION CROSS SECTIONS AND KINEMATICS

Table 1 shows the reactions which contribute to the DTS detector response, including the Q value and the first and second reaction thresholds

The reaction cross sections were considered to be zero below the second reaction threshold All cross section values were taken from the ENDF/B-V evaluation [8,16] Intermediate values to those contained in the cross section tables are obtained by linear interpolation, for all reactions involved The tables contain mesh points apropriate to the cross section structure in order to minimize interpolation errors, mainly near the carbon resonances

The angular distribution for the elastic scattering on hydrogen, H(n,n)H, was obtained from Hopkins and Breit [10] The center-of-mass scattering angle θ is selected by simulating a differential cross section experiment [15] For this purpose the angular distribution is normalized at $\cos\theta = 1$

$$F(\cos\theta') = \frac{\sigma(\cos\theta')}{\sigma(1,0)} = \sum_{l=0}^{n} \Omega_l P_l \qquad (1)$$

A value for $\cos\theta'$ is chosen at random in the [-1,1] interval Then a number R is chosen at random in the (0,1] interval If F>R then the trial is accepted and the scattered neutron energy is given by :

$$E = \frac{E}{2}\,[1 + \cos\theta'] \qquad (2)$$

Table 1 Reactions which contribute to the Dual Thin Scintillator (DTS) detector response

Reaction	Q (MeV)	1st Threshold (MeV)	2nd Threshold (MeV)
$^{1}H(n,n)^{1}H$	-	-	-
$^{12}C(n,n)^{12}C$	-	-	-
$^{12}C(n,n'\alpha)^{12}C$	-4 433	4 805	5 840
$^{12}C(n,\alpha)^{9}Be$	-5 704	6 183	6 428
→ $^{8}Be + \alpha$	+0 289	-	-
→ 3α	+0 102	-	-

where E is the incident neutron energy Equation (2) can be used for both non-relativistic and relativistic cases

The recoil proton energy is given by .

$$E_p = E - E' \qquad (3)$$

The angular distribution data for the elastic scattering on carbon, C(n,n)C , has been obtained from ENDF/B-V Since the coefficients for the expansion in Legendre polynomials are given for the center-of-mass system, it was necessary a transformation to the laboratory system in order to be compatible with the Monte Carlo code This transformation has been performed using the following relationship

$$w_l = \Sigma\, U_{lm}^{*}\, w'_l \qquad (4)$$

where U_{lm} are the transformation matrix elements taken from the ENDF/B-V and w_l and w'_l are the Legendre coefficients in

the laboratory and center-of-mass systems, respectively The elements U_{lm} are related to the Jacobian for the transformation of solid angles between the two reference systems [4]

In the case of reaction C(n,n)C, the selection of the scattering angle was performed similarly to the H(n,n)H case For the accepted trial, the elastic scattered neutron energy is given by

$$E' = E\left[\frac{\cos\theta}{13} + \sqrt{\frac{11}{13} + \left(\frac{\cos\theta}{2}\right)^2}\right]^2 \qquad (5)$$

The code CARLO DTS has the option of calculating E' relativistically by the following formula ·

$$E' = \frac{E}{169}\left\{2\left[1+\frac{E}{2E_o}\right]\cos\theta\left[\cos\theta+(\cos^2\theta+143)^{1/2}\right]+143\left[1+\frac{E}{13E_o}\right]\right\} \times$$

$$\left\{1 + \frac{2E}{13E_o}\left[1 + \frac{E}{26E_o}\right] - \frac{2E}{169E_o}\left[1 + \frac{E}{2E_o}\right]\cos^2\theta\right\} \qquad (6)$$

where E_o = 939 573 MeV = neutron rest energy

The carbon recoil energy is given by ·

$$E_C = E - E' \qquad (7)$$

For the C(n,n'γ)C reaction the anisotropy in the angular distribution of scattered neutrons has been considered The Legendre coefficients were taken from reference [9] for the energy range between 8970 and 14930 keV For the remaining energy range (between 4812 and 20000 keV) the coefficients were taken from the ENDF/B-V [8] The selection of the scattering angle θ has been performed similarly to the H(n,n)H case For the accepted trial the energy of the inelastically scattered neutron was

calculated in the center-of-mass system by the following non-relativistic approximation :

$$E' = E\left[\frac{145}{169} + \frac{156}{169}\frac{Q}{E} + \frac{24}{169}\cos\theta'\left(1 + \frac{13}{12}\frac{Q}{E}\right)^{1/2}\right] \qquad (8)$$

After calculating E', the scattering angle θ' has been converted to the laboratory angle θ :

$$\cos\theta = \left(1 + 12\cos\theta' S_Q\right) / \left(145 + 144\, S_Q^2 + 24\cos\theta' S_Q\right)^{1/2} \qquad (9)$$

where $S_Q = \left(1 + \frac{13}{12}\frac{Q}{E}\right)^{1/2}$

The carbon recoil energy is given by :

$$E_C = E - E' - Q \qquad (10)$$

The detection of gamma-rays from $^{12}C(n,n'\gamma)^{12}C$ reaction has been calculated separately by means of a simplified Monte Carlo code as described in reference [2]. The results of the correction factor due to this effect are shown in Table 2 for a neutron beam incident on the detector axis For finite beam sizes the correction tends to be lower

The angular distribution of alphas from the $^{12}C(n,\alpha)^{9}Be$ reaction has been considered as isotropic in the Laboratory system This simplification has very little effect on the results since the discrimination level of the proton-recoil spectrum can always be chosen above the channel corresponding to the maximum energy of the alpha particles produced by this reaction

Table 2 Results of the correction factor due to the detection of gamma-rays from $^{12}C(n,n'\gamma)^{12}C$ reaction

Energy (keV)	Correction Factor	Energy (keV)	Correction Factor
4850	1 0000	6540	1 0025
4930	1 0003	6640	1.0017
4980	1 0005	7180	1.0015
5100	1 0004	8044	1 0037
5180	1 0004	9000	1 0022
5280	1 0009	10000	1.0024
5380	1 0014	11000	1 0024
5550	1 0012	12224	1 0014
5900	1 0019	13250	1 0012
6250	1 0025	14000	1.0010
6350	1 0031	14750	1 0008
6410	1 0024	15477	1 0007

The angular distribution of alphas from the $^{12}C(n,n')3\alpha$ reaction has been considered as isotropic in the Laboratory system The Q value for this reaction has been determined considering all the excitation energy levels, real or virtual, contained in the ENDF/B-V [8] For each neutron energy a set of excitation probabilities values, P_i, has been generated for the compound nucleus states This probability is the ratio between the partial cross section for a given excitation state and the total cross section for that neutron energy These cross section values were also obtained from ENDF/B-V The excitation state is selected by comparing P_i with a random number R between (0,1) If $R<P_i$ the level is accepted and Q is given by the i-th value in table 3

Table 3 $^{12}C(n,n')3\alpha$ reaction Q values for different excitation levels of the $(^{12}C + n)^*$ compound nucleus.

level index	Q value (keV)	level index	Q value (keV)
1	7275	10	13250
2	7655	11	13750
3	9638	12	14250
4	10300	13	14750
5	10840	14	15250
6	11250	15	15750
7	11750	16	16250
8	12250	17	16750
9	12750	18	17250

3 2 Application of the forced first collision technique

This technique allows a reduction in the number of histories followed by the Monte Carlo code, without significant loss in the statistical accuracy achieved. It was used to define the point where the first neutron collision will occur or to make the neutron collide preferentially with the hydrogen atoms in the scintillator

The use of this technique is optional in the code Carlo DTS depending on the input parameters However, its use is obligatory in case of item 3 2 1 described below, in order to avoid too large a number of incident neutrons necessary to obtain statistical errors of < 0 5%

3 2 1 Forced first collision inside the detector

The DTS detector has high transmission for MeV

neutrons, and consequently a low detection efficiency Therefore a great number of incident neutrons should be necessary to get a low statistical uncertainty, demanding a long processing time This problem has been solved by using the forced first collision technique In this case, the neutron first collision is confined inside the detector and the distance to the first collision point is given by [1]·

$$\ell = - \lambda \, ln\left\{1 - R\left[1 - \exp(-L/\lambda)\right]\right\} \qquad (11)$$

where·

$\lambda = 1/\Sigma_T$ = average distance to the first collision, R is a random number in the [0,1] interval

and

$L = H_T$ is the total thickness of the DTS detector $(0 < \ell < L)$

This procedure results in a 100% detection efficiency The reduction in the processing time reaches a factor around 20 at 15 MeV To the calculated efficiency the following detection factor must be applied :

$$D = [\ 1 - \exp\ (-L/\lambda)] \qquad (12)$$

The distance to subsequent collisions are calculated by the usual formula

$$\ell = - \lambda \, ln\ R \qquad (13)$$

3 2.2 Forced first collision on hydrogen and ZONE 1

Table 4 shows the percentage contribution in the DTS detector efficiency from events originated by neutron first collision on hydrogen and carbon for different neutron energies Between 89-96% contribution comes from events where the first neutron collision was on hydrogen

Table 4 Contribution to the DTS detection efficiency of events originated by neutron first collision on hydrogen, carbon and ZONES 1 and 2 (in percent)

Neutron Energy (MeV)	Contribution to the Efficiency (%)			
	Hydrogen	Carbon	ZONE 1	ZONE 2
1 0	89 0	11 0	95 6	4 4
2 4	93 8	6 2	96 7	3 3
14 0	96 4	3 6	98 6	1 4

Since the ratio between the total cross sections of hydrogen and carbon are in the range of 0 5 to 3, for 1 to 15 MeV neutrons, the fraction of neutrons which have first collision on hydrogen is between 30 and 77 % Therefore, it becomes convenient to force the first collision on hydrogen in order to reduce the processing time by a factor up to about 3

A fraction f_H of the incident neutrons is forced to collide against hydrogen and $(1 - f_H)$ collide against carbon atoms The number of counts in the proton-recoil

spectrum becomes real numbers X given by

$$X = \begin{cases} 1 & \text{(hydrogen)} \\ \dfrac{f_H}{(1 - f_H)} \left(\dfrac{\Sigma_T}{\Sigma_H} - 1 \right) & \text{(carbon)} \end{cases} \qquad (14)$$

The number of processed neutrons, N_s, gives rise to a larger number of counts in the proton-recoil spectrum, N'_s, given by :

$$N'_s = f_H \frac{\Sigma_T}{\Sigma_H} N_s \qquad (15)$$

The processing time is reduced by the factor N'_s / N_s. At 14 MeV and using $f_H = 0\ 9$, this factor is equal to 2 4

As shown in table 4, between 95 to 99 % of the counts which contribute to the efficiency are originated by a neutron first collision in the first scintillator (ZONE 1) Because of the high transmission through the detector for 1 to 15 MeV neutrons, about half of the neutrons are incident in ZONE 1 and half are incident in ZONE 2 Therefore applying the forced first collision in the first scintillator (ZONE 1) it is possible to reduce the processing time by a factor of 2

A fraction f_s of the incident neutrons is forced to collide in ZONE 1 and $(1 - f_s)$ collide in ZONE 2 The counts in the proton-recoil spectrum becomes

$$X = \begin{cases} X & \text{(scintillator 1)} \\ X \ \dfrac{f_s}{1 - f_s} \ (P/P_1 - 1) & \text{(scintillator 2)} \end{cases} \qquad (16)$$

where

$$P = 1 - \exp\ (-\Sigma_T\ H_H) \quad \text{and}$$

$$P_1 = 1 - \exp\ (-\Sigma_T\ H_1)$$

The number of processed neutrons N'_s gives rise to a larger number of counts, given by

$$N''_s = N' f_s \frac{P}{P_1} \qquad (17)$$

The processing time is reduced by the factor N''_s/N'_s. The total reduction, including the forced collision on hydrogen becomes N''_s/N_s At 14 MeV and using $f_s = f_H = 0\ 9$, the total reduction is 4 3

3 3 Pulse height distribution

The light yield produced by protons, alpha particles and carbon or beryllium nuclei, are obtained by interpolation in a light table [17] The light produced by beryllium and carbon nuclei are considered to have the same value For each interaction during the neutron history, the light yield produced by all particles is accumulated, giving rise to a count in the pulse height spectrum on a channel proportional to the total light produced by the neutron

The CARLO DTS code calculates two types of pulse height spectra In the first, all neutron interactions inside the DTS detector are included and the proton escape effect is not considered In the second, a distiction is made between the histories which start with a neutron interaction in ZONE 1 and those histories started in ZONE 2 In this case, only those histories that produce a pulse height in the first scintillator above the electronic discrimination level are computed in the final spectrum Moreover, the effect of escape of protons from the scintillators and the geometrical variation in the light collection are also taken into account This second calculated pulse height spectrum is much more realistic and is the one used in the comparisons with the experimental spectra and for the determination of the theoretical

efficiency for the DTS detector

The NE-110 plastic scintillator, used in the DTS detector, has a light response slightly different as compared to NE-213 from which the light table was taken [17] For this reason, the experimental determination of the light yield for protons in NE-110 scintillator has been performed Details of this light yield measurement are described in reference (2)

Once the pulse height table, as a function of the proton energy, has been obtained, the output proton recoil spectrum from the CARLO DTS code was converted into a new spectrum according to this new pulse height table This conversion procedure was performed with a resolution equivalent to 1/50 of a channel, keeping constant the total number of counts in the spectrum This procedure takes into account possible non-linearity in the electronics

3.4 Lost coincidences effect

For MeV neutrons, there is a large effect due to the escape of protons from the forward face of the first scintillator in the DTS detector However, the corresponding distortion in the proton recoil spectrum is eliminated experimentally by detecting these escaped protons at the second scintillator, placed behind the first one Since this procedure requires a coincidence signal, there is a lower limit for the first scintillator pulse amplitude to be detectable The sum-coincidence pulses originated from pulses in the first scintillator below this limit will be lost Some of these lost sum-coincidence pulses can have an amplitude above the discrimination level adopted for the detection efficiency calculation (usually 30 % of the maximum proton energy) Therefore, a correction for these lost coincidences is required At low neutron energies there are sum-coincidence pulses also due to neutron multiple scattering inside the scintillators The loss of such events

must be taken into account

The lost coincidences effect caused by the escape of protons has been incorporated in the CARLO DTS code, by calculating the proton energy fraction deposited inside each scintillator

First, the proton directional coordinate along the z axis, w_p, has been evaluated ·

$$w_p = w\left(\frac{E}{E_p}\right)^{1/2} - w'\left(\frac{E'}{E_p}\right)^{1/2} \qquad (18)$$

where·

w and w′ are the neutron directional coordinates, before and after the scattering, respectively.

E and E′ are the neutron energy, before and after the scattering, respectively, and

E_p is the recoil proton energy

Then, the proton range in scintillator NE110 has been evaluated by the following equation

$$R_p = \exp\left[f(E_p)\right] \qquad (19)$$

where·

$$f(E_p) = \sum_{i=0}^{6} a_i \left[\ln(E_p)\right]^i \qquad (20)$$

The coefficients a_i were obtained by a weighed least square fitting, from the range as a function of the energy obtained by Janni [1], for the energy interval between 1 keV and 20 MeV The weights applied to the points followed the usual rule

$$w = \left[\frac{1}{\sigma_{\ln R}}\right]^2 = \left[\frac{100}{\sigma_{R(x)}}\right]^2 \qquad (21)$$

The results of a_1 are shown on table 5

The Z coordinate of the proton has been determined from its range at the end point of the proton path ·

$$Z'_p = Z_p + W_p R_p \qquad (22)$$

The fraction of the proton path which is contained within the first scintillator is given by

$$R_2 = R_p(Z'_p - H_1)/(Z'_p - Z_p) \qquad (23)$$

The remaining energy of the proton as it leaves the first scintillator, E_2, is calculated from its range R_2 by the following equation

$$E_2 = \exp\,[g(R_2)] \qquad (24)$$

where

$$g(R) = \Sigma\, b_i\, [\ln(R)]^i \qquad (25)$$

The values of b_i were obtained similarly as a_i In this case, the weight applied to the points has been calculated by an iterative procedure [5], given by

$$L = \frac{w_x}{F_x^2} \qquad (26)$$

where

$$F = y - \sum_{i=0}^{6} b\,(x)$$

and

$Y = \ln E$, $x = \ln R$, $F_x = \partial F/\partial x$ and $w_x = 1/\sigma^2$

The results of b_i are also shown in table 5

Table 5 Coefficients from least square fits of range vs proton energy (a_i) and of proton energy vs range (b_i) (E in MeV, R in μm)

Index	a_i	b_i
0	3 1132	2 5148
1	1 6048	1 1361
2	9 8827 E-2	1.3538 E-1
3	- 2 4682 E-2	1.8243 E-4
4	- 1 3069 E-3	5 0465 E-3
5	9 4840 E-4	7 6368 E-4
6	8 7869 E-5	3.4953 E-5

The observed residues in the fitting of the proton range as a function of the energy were always lower than the uncertainties of the ranges in the table The same has been observed for the inverse relationship, proton energy as a function of its range For proton energies above 500 keV, these residues were less than 1 % A correction has been applied to the resulting ranges, in order to account for the difference between the densities of NE110 and the scintillator PILOT B, for which the table used is applicable

For proton energies below 10 keV the range is less than 3×10^{-5} cm For this reason, the proton range has been considered zero below this energy, in order to reduce the CARLO DTS processing time

For those events where the proton escapes depositing part of its energy in the second scintillator (by multiple scattering), the fraction of the trajectory which is outside the detector is given by .

$$E_1 = E_p - E_2 \qquad (27)$$

For events where a coincidence takes place, but the proton recoil is produced in the second scintillator (by multiple scattering), the fraction of its trajectory which escapes the detector is given by

$$R_2' = R_p \, (Z_p' - H_T)/(Z_p' - Z_p) \qquad (28)$$

corresponding to the energy

$$E_2' = \exp [g(R_2')] \qquad (29)$$

In this case, the contribution to the spectrum is given by the fraction of the proton energy which is deposited in the second scintillator, as follows

$$E_2 = E_p - E_2' \qquad (30)$$

The total light produced by a given neutron in the Monte Carlo code has been divided into two parts: the first one corresponds to the total light produced in the first scintillator (ZONE 1) and the second one corresponds to the total light produced in the second scintillator (ZONE 2) The events which produce a light yield below a given threshold are rejected In this way, the loss of coincidences caused by multiple scattering are also included

The code CARLO DTS can obtain the correction for lost coincidences for any value of the discriminator lower level by means of the array NCOIN(I) In this array are the

counts from pulses produced in the first scintillator, whose amplitudes when added to those produced in the second scintillator - for the same neutron - results in amplitudes above the channel corresponding to 30% of the maximum proton energy

The correction for lost coincidences are shown in fig 4 as a function of the fractional discriminator lower level (ratio between the channel at the discriminator lower level and the channel at the end of the spectrum), for several energies of the incident neutron In this figure, the discrimination level adopted for the calculated efficiency corresponds to 30% of the maximum proton energy

3 5 Variation in light collection

The variation in the light collection efficiency at different points in the scintillator has been taken into account by the following relationship

$$P(r) = P(0)\ (1 + ar^2) \qquad (31)$$

where P(r) is the average light response at distance r (in cm) from the center of the scintillator For the detector described in reference [3], the measured values of a were 0 0107 and 0 0040 for the first and second scintillators respectively

4 RESULTS OF THE CALCULATIONS

4 1 DTS neutron detection efficiency

The behavior of the calculated biased efficiency with neutron energy is shown in fig 5 together with two experimental points obtained at 2 446 MeV and 14 04 MeV [3] The curve follows essentially the H(n,n)H cross section Contributions from C(n,n)C and $^{12}C(n,n'\gamma)^{12}C$ cross sections

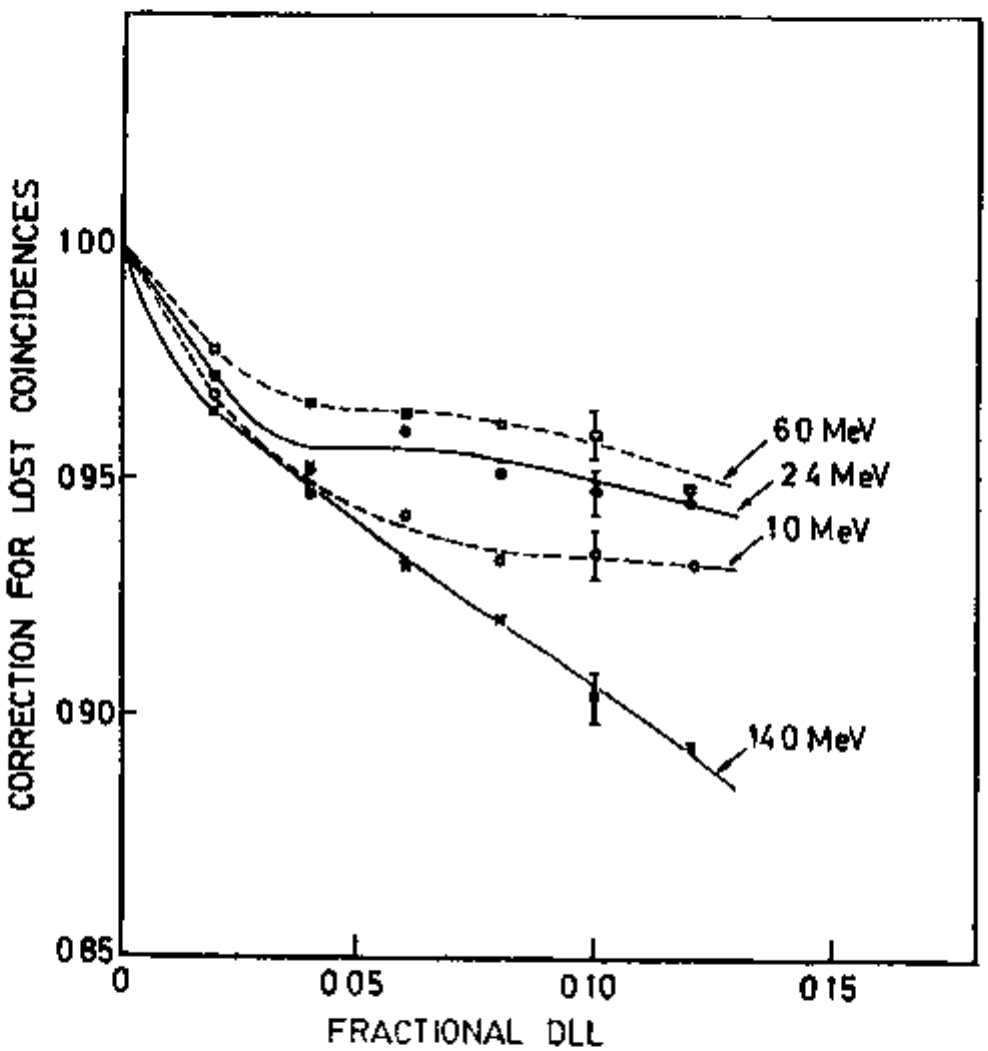

FIGURE 4 - Lost coincidences correction as a function of the fractional lower discrimination level

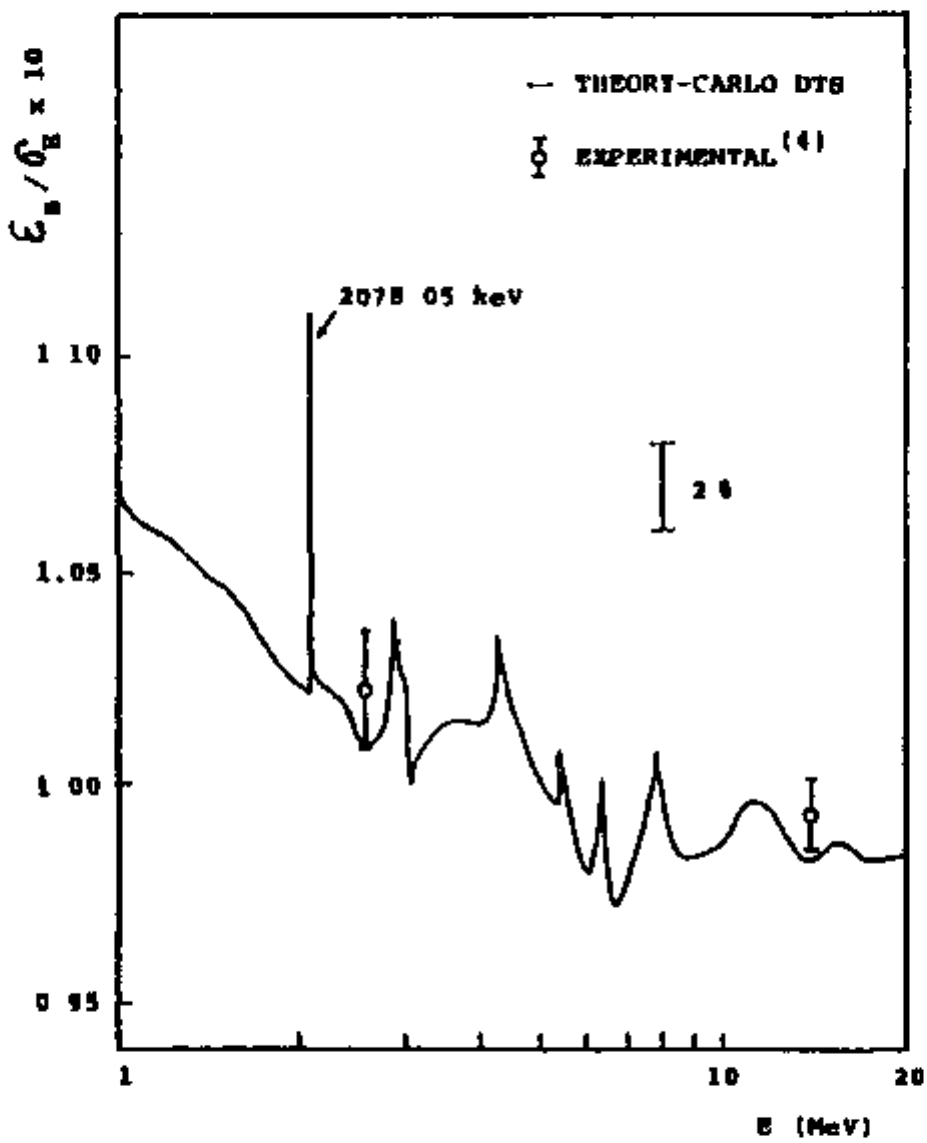

FIGURE 5 - DTS efficiency curve for 1 to 20 MeV neutrons Spectrum bias at 30% of the maximum energy The points at 2 446 and 14 04 MeV were obtained experimentally The solid line is the Monte Carlo calculation

cause some small irregularities in the efficiency curve, mainly in the regions of carbon resonances For this curve, the bias energy was located at 30% of the maximum energy

A clear correlation between the biased efficiency and the carbon and hydrogen cross section has been observed Particularly, good accuracy in the interpolation of the efficiency for various neutron energies was achieved by the following formula

$$\varepsilon_B/\sigma_H = a_1 + a_2\sigma_c + a_3\sigma_H \qquad (32)$$

where

ε_B is the biased efficiency,

σ_c is the carbon elastic plus inelastic scattering cross sections,

σ_H is the H(n,n)H cross sections, a_1, a_2, a_3 are constants

The values of a_1, a_2 and a_3 were obtained by least squares fit between the biased efficiency and the cross sections The efficiency has been calculated at several selected neutron energies, at points where the carbon cross section shows the largest variations Updated results of the fits are presented in table 6 for three fractional bias energies, namely 0 30, 0 35 and 0 40 of the maximum energy These efficiencies were calculated at zero discrimination lower level The average accuracy obtained in the interpolation goes from 0 8 to 1 8% at the fractional biases of 0 30 and 0 40, respectively

Table 6 Coefficients of the interpolation formula applicable to the DTS biased efficiency

fractional bias energy	a_1 ($\times 10^{-3} b^{-1}$)	a_2 ($\times 10^{-4} b^{-2}$)	a_3 ($\times 10^{-4} b^{-3}$)	reduced chi square
0 30	9 474	1 901	1 576	1 04
0 35	8 798	1 664	1 710	1 19
0 40	8 134	1 522	1 719	1 10

The value of a_1 corresponds to the biased efficiency without the multiple scattering correction, in b^{-1} The values of a_2 and a_3 correspond to the multiple scattering correction in carbon and hydrogen, respectively, in b^{-2}. The values of a_2 decreases with the fractional bias energy, whereas a_3 increases This behavior is explained by the variation in the spectrum shapes due to multiple scattering For carbon, the counts are shifted to lower pulse amplitudes, whereas for hydrogen, the counts are shifted to higher pulse amplitudes [12]

The interpolation formula described above does not take into account variations in the efficiency caused by angular anisotropy in C(n,n)C , H(n,n)H and $^{12}C(n,n'\gamma)^{12}C$ reactions For this reason, in applications where the highest accuracy is desirable it is preferable to interpolate on parameter ϵ_B/σ_H, as a function of the neutron energy Moreover, the ENDF/B-VI data file should be used for the H(n,n)H cross section

Figure 6 shows the uncertainties involved in the

calculated efficiency The uncertainty indicated for the H(n,n)H cross section has been taken from ENDF/B-VI (0 3%) The predominant contributions to the total uncertainty are from the hydrogen areal density and statistics in the calculation, except near the carbon resonance at 2078 keV where the multiple scattering uncertainty is predominant

The uncertainty in the correction for lost coincidences has not been included in fig 6 since it depends on the discrimination level used This uncertainty is estimated to be around 10% of the correction (i e 0 4%) and has little contribution in the total uncertainty The total uncertainty is between 0 8 to 1 0% except near the carbon resonance at 2078 keV, where it reaches the maximum value of 1 2%

4 2 Proton recoil spectra

The comparison between the results of proton recoil spectra calculated by the code CARLO DTS, in comparison to experimental spectra obtained at 2 446 MeV and 14 04 MeV, can be seen in figures 7 and 8 The fitting between the calculated and the experimental spectra was performed using a revised version of a code written by Meier [13], which takes into account the Poisson statistics in the number of photoelectrons detected The agreement between the calculated and the experimental spectrum shapes was excellent, indicating little sensitivity with respect to the selected bias energy

5 DTS AS A NEUTRON SPECTROMETER

In the present work the DTS neutron detector has been used to measure neutron fluence However, it can also be used as a neutron spectrometer In this mode, only coincidence pulses are registered resulting in a peak-shaped pulse height spectrum as shown in figure 9 This spectrum

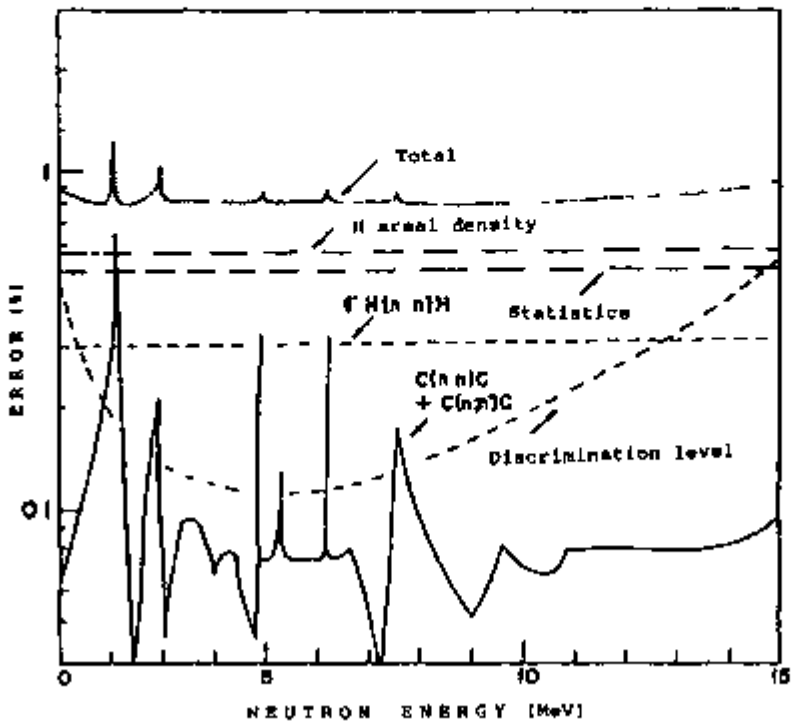

FIGURE 6 - Uncertainties in the CARLO DTS efficiency calculation

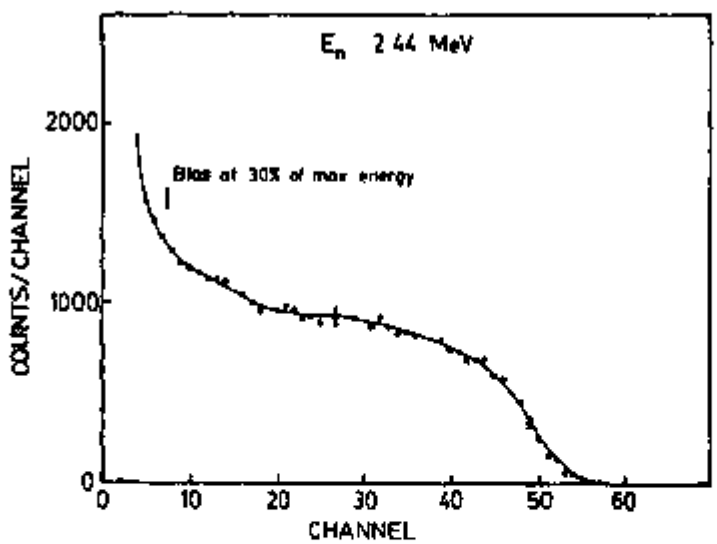

FIGURE 7 - Comparison between experimental (dots) and calculated proto-recoil spectra (solid line) at 2 446 MeV neutron energy

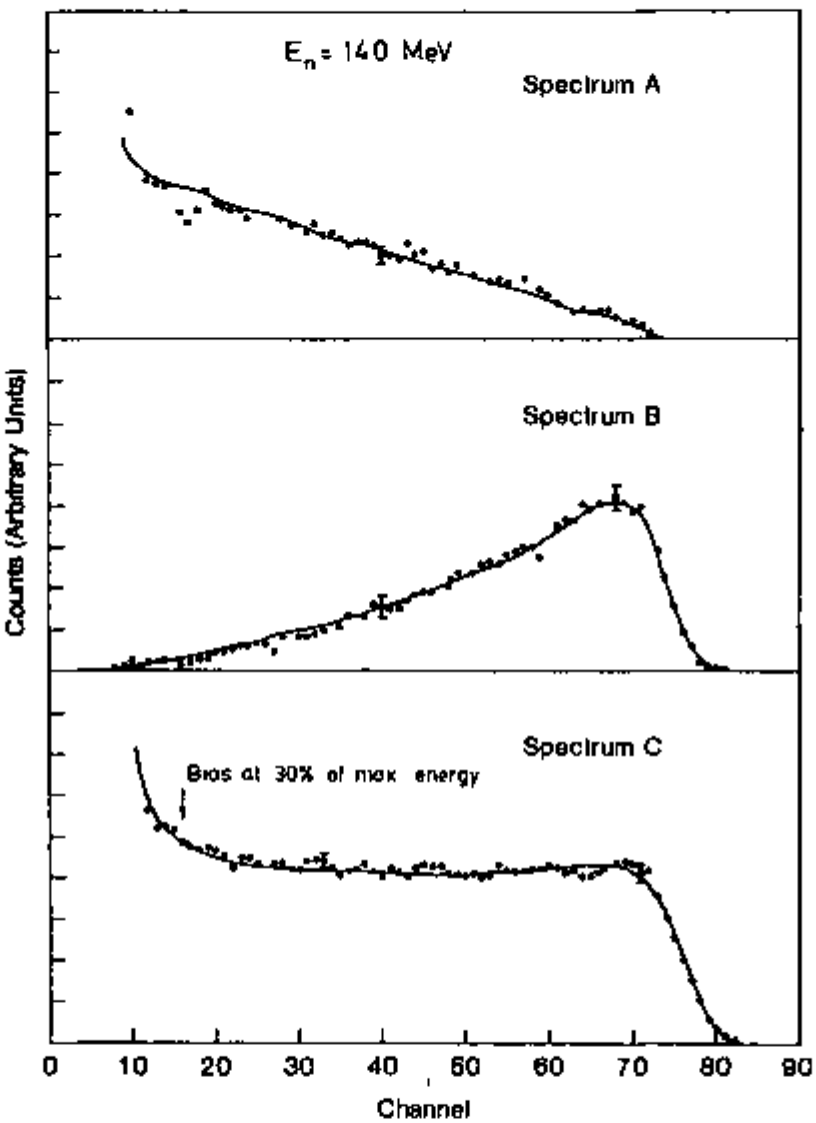

FIGURE 8 - Comparison between experimental (dots) and calculated proton-recoil spectra (solid line) at 14 04 MeV neutron energy In this figure spectrum A corresponds to singles from the first scintillator, spectrum B are coincidences between the two scintillators and spectrum C is the sum spectrum which approximates the ideal thin scintillator response

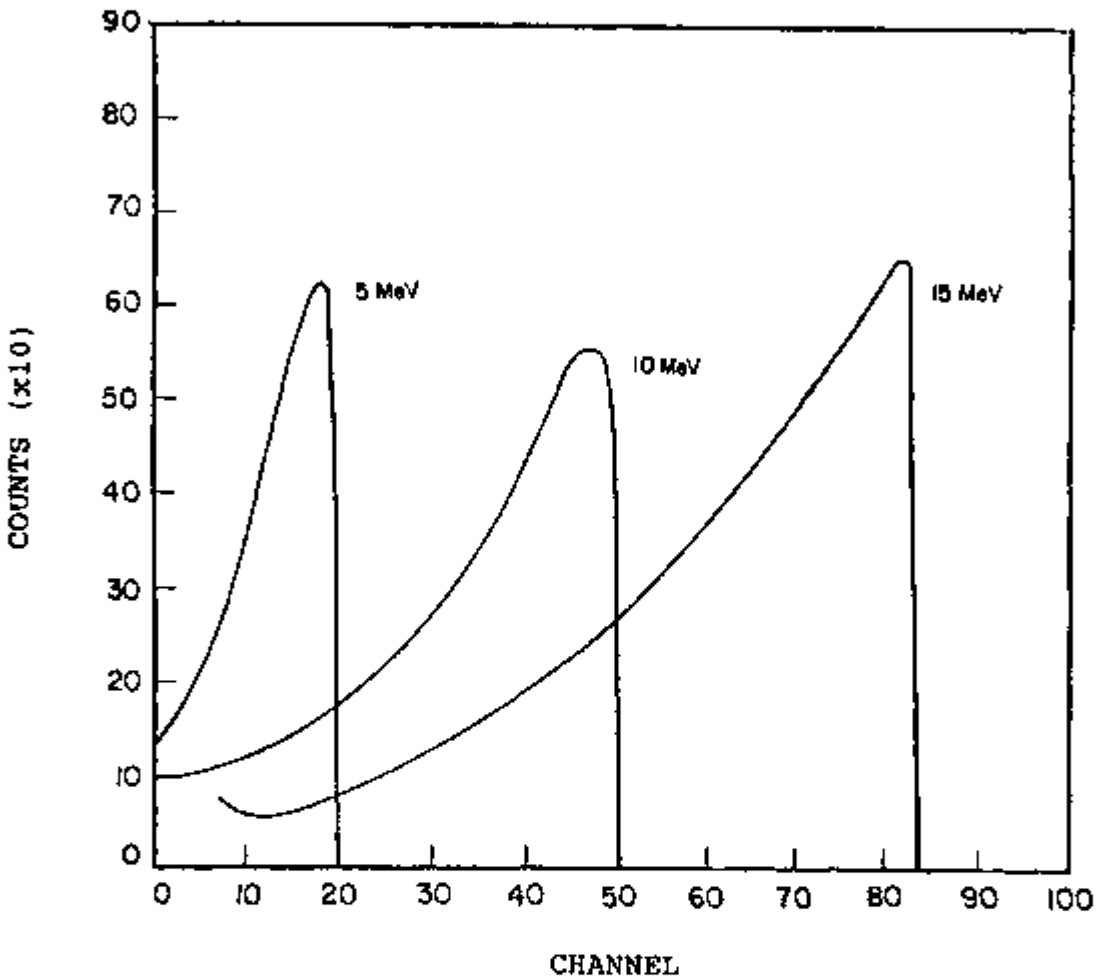

FIGURE 9 - Monte Carlo calculations of the DTS coincidence spectrum for different neutron energies

shape is desirable because it allows a better separation between different energy components of a complex neutron spectrum At high neutron energies this peak-shaped spectrum is due to the escape of protons from the forward edge of the first scintillator At lower energies the peak still exists but it is not so well defined In this case, it is produced by neutron multiple scattering The code CARLO DTS can calculate the coincidence spectrum by selecting the corresponding option

The possibility of using the DTS detector as a neutron spectrometer has been investigated by Duvall and Johnson [6,7]

6 CONCLUSION

The Monte Carlo code called CARLO DTS provides efficiency and proton recoil spectrum calculation for the Dual Thin Scintillator (DTS) neutron detector in the energy range from 1 to 20 MeV The code takes into account the effect of the escape of protons from the scintillators and makes use of forced collision techniques in order to reduce the processing time The overall uncertainty in the calculated efficiency is between 0 8 to 1 0% in the 1-15 MeV range except near the carbon resonance at 2078 keV, where it reaches the maximum value of 1 2% The uncertainties are lower than reported previously due to improvements performed in the code and to the use of updated H(n,n)H cross section values The agreement between calculated and experimental spectrum shapes at two neutron energies, 2 446 and 14 04 MeV, was excellent, indicating little sensitivity with respect to the selected bias energy The DTS neutron detector can be also used as a neutron spectrometer In this mode, only coincidence pulses are counted The resulting peak-shaped pulse height spectrum is convenient for unfolding complex neutron spectrum This feature has been incorporated in the code CARLO DTS

The code CARLO DTS has been written in FORTRAN language A copy of the code as well as running details are available from the author

7 ACKNOWLEDGMENTS

The author would like to thank the staff of the Neutron Interactions and Dosimetry group from the National Institute of Standards and Technology (NIST) - USA, for the support to the present work He is specially indebted to Dr Ronald G Johnson for his valuable discussions and to his calculation of the $^{12}C(n,n')3\alpha$ reaction Q values (Table 3)

REFERENCES

01 CASHWELL, E D & EVERETT,C J A practical manual on the Monte-Carlo method for random walk problems. New York, Pergamon, 1959

02 DIAS, M S Desenvolvimento e aplicação de um detector para a medida absoluta da taxa de fluência de nêutrons na região de MeV. São Paulo, 1988 (Tese de doutoramento, Instituto de Pesquisas Energéticas e Nucleares)

03 DIAS, M S , JOHNSON, R G , WASSON,O A Design and calibration of an absolute flux detector for 1-15 MeV neutron Nucl. Instrum. Methods Phys. Res., A 224, 532-46, 1984

04 DIAS, M S , CARLSON, A D , JOHNSON, R G , WASSON, O A Application of the dual thin scintillator neutron flux monitor in a ^{235}U (n,f) cross-section measurement In INTERNATIONAL ATOMIC ENERGY AGENCY Nuclear standard reference data, proceedings of an Advisory Group meeting, held in Geel, Nov. 12-16, 1984 Vienna, 1985 p 467 (IAEA-TECDOC-335)

05 DEMMING, W E Statistical adjustment of data. New York, Wiley, 1948

06 DUVALL,K C & JOHNSON,R G The development of the dual thin scintillator (DTS) in the 1+2 coincidence configuration as a neutron spectrometer Radiat Eff , 95(1/4) 319, 1986

07 DUVALL,K C & JOHNSON,R G Monte Carlo calculation of the dual-thin scintillator neutron detector in the

sum-coincidence mode of operation In Nuclear Data for Science and Technology international conference on , held in Mito, May 30 - June 3, 1988

08 FU, C Y & PEREY, F G Summary documentation for carbon (MAT 1306) In KINSEY, R comp ENDF-201 ENDF/B summary documentation. Upton, N Y , Brookhaven National Laboratory, Jul 1979 (BNL-NCS-17541 (ENDF-201) Ed 3 (ENDF/B-V))

09 GLASGOW, D W , PURSER, F O , HOGUE, H , CLEMENT,J C , STELZER, K , MACK, G ; BOYCE, J R , EPPERSON, D H , BUCCINO, S G , LISOWSKI, P W , GLENDINNING, S G , BILPUCH, E G , NEWSON H W , GOULD, C R Differencial elastic and inelastic scattering of 9 to 15 MeV neutrons from carbon Nucl. Sci. Eng., 61 521-33 1976

10 HOPKINS, J C & BREIT, G $^{1}H(n,n)^{1}H$ scattering observables required for high precision fast-neutron measurements Nucl. Data Tables, A9 137, 1971

11 JANNI, R F Proton range-energy tables, 1 KeV-10 GeV Part 1 Compounds At. Data Nucl. Data Tables, 27 (2/3) 147, 1982

12 JONES, D W & TOMS, M E A neutron spectrometer using organic scintillators. Washington, D C , Naval Rese a rch Laborato r y, Nov 1971 (NRL-Report-7324)

13 MEIER, M M Data reduction programs for Harris computer Washington, D C , U S National Bureau of Standards, Feb 19, 1978 (NBS internal report,

Rev set 1984)

14 MONAHAN,J Kinematics of neutron producing reacting In MARION, J B & FOWLER, J L Eds Fast Neutron Physics Part I. Techniques. New York, Interscience, 1960 sec 1, p 49

15 POENITZ, W P The black neutron detector. Argonne, Ill , Argonne National Laboratory, 1972 (ANL-7915)

16 STEWART, L , LABAUVE, R J , YOUNG, P G Summary documentation for ^{1}H (MAT 1301) In KINSEY, R , comp ENDF 201. ENDF/B summary documentation. Upton, NY, Brookhaven National Laboratory, Jul 1979 (BNL-NCS-17541 (ENDF-201 3,ed (ENDF/B-V)

17 TEXTOR, R E & VERBINSKI, V V 05S. a Monte-Carlo calculation of the pulse height distributions for monoenergetic neutrons on organic scintillator systems Oak Ridge, TN, Oak Ridge National Laboratory, Feb 1968 (ORNL-4160)